We have also quenched $Rh_2(TMB)_4^{2+*}$ ($^3A_{2u}$) with PQ^{2+} in methanol. Excitation at wavelengths longer than 450 nm produces the transient spectrum shown in Figure 3. The absorption features at wavelengths greater than 600 nm and near 395 nm are attributed mainly to $PQ^{\cdot+}$.[26] The bleaching near 515 nm and the absorption at 450 nm are from the binuclear rhodium complex. We attribute the 450-nm absorption to the one-electron-oxidized rhodium species, $Rh_2(TMB)_4^{3+}$; the back-reaction between $Rh_2(TMB)_4^{3+}$ and $PQ^{\cdot+}$ obeys second-order kinetics (k_b = (2.2 ± 0.5) × 10^8 M^{-1} s^{-1} (21 °C) (μ = 1.95 × 10^{-2} M). We have previously shown[5,6] that flash photolysis of $Rh_4(br)_8^{6+}$ in 1 N H_2SO_4 leads to transient production of $Rh_2(br)_4^{3+}$. The difference spectrum in this case is dominated by bleaching of the ground-state absorption and a large absorption peak at 440 nm. The intensity and shape of this absorption band are very similar to those associated with the peak at 450 nm attributed to $Rh_2(TMB)_4^{3+}$, providing further confirmation that the transient comes simply from one-electron oxidation of $Rh_2(TMB)_4^{2+*}$ ($^3A_{2u}$).

Flash photolysis of $Rh_2(br)_4^{2+}/PQ^{2+}$ in acetonitrile solution produced a transient spectrum (50 μs after the flash) that is very similar to that of the $Rh_2(TMB)_4^{2+}/PQ^{2+}$ system in methanol; the absorption maximum of $Rh_2(br)_4^{3+}$ is at 435 nm and bleaching is observed at 550 nm. However, in this system the kinetics are very complex, owing to the fact that $Rh_2(br)_4^{3+}$ can react with itself or with $Rh_2(br)_4^{2+}$ to give $Rh_4(br)_8^{n+}$ (n = 5, 6).[6] These Rh–Rh bond-forming reactions compete with electron back-transfer and thus give secondary products which themselves eventually react with $PQ^{\cdot+}$ to give $Rh_2(br)_4^{2+}$ and PQ^{2+}. In the case of $Rh_2(TMB)_4^{2+}$, the methyl groups on the ligand inhibit association of the partially oxidized binuclear species,[7] and electron back-transfer predominates.

Acknowledgment. S.J.M. acknowledges a Chaim Weizmann Fellowship (1979–1980). We thank Johnson Matthey, Inc., for a generous loan of rhodium trichloride. This research was supported by National Science Foundation Grant No. CHE78-10530.

(26) For $PQ^{+\cdot}$, ϵ(395 nm) = 2.9 × 10^4 M^{-1} cm^{-1} (Kosower, E. M.; Cotter, J. L. *J. Am. Chem. Soc.* **1964**, *86*, 5224).

Thermochemistry and Dissociation Dynamics of State-Selected C_4H_4X Ions. 1. Thiophene

James J. Butler and Tomas Baer*

Contribution from the Department of Chemistry, The University of North Carolina at Chapel Hill, Chapel Hill, North Carolina 27514. *Received January 29, 1980*

Abstract: The threshold photoelectron spectrum of thiophene and photoionization efficiency curves for $C_4H_4S^+$, $C_4H_3S^+$, C_3HS^+, $C_2H_2S^+$, CHS^+, and $C_3H_3^+$ from thiophene were measured in the 8–14-eV photon energy range. $C_2H_2S^+$ is the only fragment produced below 12.9 eV, and its thermochemical dissociation onset was determined to be 12.1 ± 0.1 eV. The dissociation rates of internal energy selected thiophene ions in the 12–12.6-eV photon energy range were determined by photoion–photoelectron coincidence (PIPECO). In addition, the average kinetic energy released in the dissociation to $C_2H_2S^+$ and C_2H_2 was determined in the 13–14-eV photon energy range. The ion lifetimes and kinetic energy release results were compared to predictions of the statistical theory (RRKM/QET). Good agreement between measured and predicted lifetimes was noted when a linear $C_4H_4S^+$ transition state and product $C_2H_2S^+$ ion were assumed. The measured kinetic release is approximately twice that predicted by the quasi-equilibrium theory.

Introduction

The gas-phase chemistry of ions has been an active area of research ever since the advent of mass spectrometry. An important goal has been the elucidation of the dissociation mechanisms of highly excited ions in order to predict the structure of the neutral precursor molecule from the distribution of fragment ions observed in a mass spectrometer.

The study of gas-phase ions is also of interest in its own right and because it makes possible comparisons between the reactions of gas-phase ions and those of ions in solution. Two major differences between these two phases are the stability and deexcitation of ions. In solution, ions are stabilized by solvation and any excited states are rapidly deexcited by collisions. On the other hand, ions in a mass spectrometer are often formed in excited states at low pressures and lose their energy primarily via unimolecular processes such as fluorescence or dissociation. As a result, one of the problems in studying gas-phase ion chemistry in conventional mass spectrometers is the broad and generally unknown distribution of internal energy of the ions.

A major advance in our understanding of ionic dissociations was the application of the statistical theory called the quasi-equilibrium theory (QET)[1] to reactions occurring in the mass spectrometer. At about the same time and independently, Marcus and Rice[2] developed an improved version of the old RRK[3] theory, which is now referred to as the RRKM theory. Although the two theories are identical in their fundamental statistical assumptions, the QET expressed its rate $k(E)$ as a function of the internal energy E while the RRKM theory went beyond this form to the thermalized rate, k(T) which is more appropriate to thermalized neutral systems. In its most basic form, the dissociation rate of a molecule (or ion) with internal energy, E, and an activation energy of E_0 is given by eq 1, where ρ and ρ^* are the density of

$$k(E) = \sigma \sum_{\epsilon=0}^{E-E_0} \rho^*(\epsilon)/h\rho(E) \quad (1)$$

vibrational and internal rotational states of the molecule (or ion) and the transition state, respectively. The parameter σ is a small number which accounts for the number of equivalent ways the molecule can dissociate and h is Planck's constant. The numerator sums over the number of energetically allowed ways of passing through the region of the transition state. This is because $E - E_0$, the energy in excess of that required to pass over the transition state, can be partitioned among the vibrational and internal ro-

(1) H. M. Rosenstock, M. B. Wallenstein, A. L. Warhaftig, and H. Eyring, *Proc. Natl. Acad. Sci. U.S.A.*, **38**, 667 (1952).

(2) R. A. Marcus and O. K. Rice, *J. Phys. Colloid Chem.*, **55**, 894 (1951).

(3) (a) O. K. Rice and H. C. Ramsperger, *J. Am. Chem. Soc.*, **49**, 1617 (1927); (b) L. S. Kassel, *J. Phys. Chem.*, **32**, 225 (1928).

0002-7863/80/1502-6764$01.00/0

tational states and the relative kinetic energy of the two dissociating fragments. The density of states, ρ, which is a strongly increasing function of the energy, can be calculated once the vibrational frequencies of the ion or the transition states are specified. These methods have been discussed by Forst.[4]

In order to apply this theory, we must know the distribution of internal energies of the system and accurate ground state and activation energies for the various reactions. Through the use of monoenergetic electron impact and photoionization measurements, a reliable set of thermochemical data is slowly being developed.[5] However, the distribution of internal energies in a conventional mass spectrometer is still largely a matter of conjecture because of a variety of complicated problems.

In order to compare experimental results with the statistical theory (or any theory for that matter), it is extremely helpful to select the internal energy of the reactant ion and to study the dissociation dynamics as a function of this internal energy. During the past decade, the technique of photoion–photoelectron coincidence (PIPECO) has been developed to accomplish this. A review of this field has recently been published.[6] It is based on eq 2 in which $h\nu$ is the energy of the photon typically 10–20 eV, $E_{th}(AB)$ is the initial thermal energy of the molecule, typically 0.050 to 0.1 eV, $E_i(AB^+)$ is the internal energy of the ion, and $KE(e^-)$ is the kinetic energy of the electron.

$$h\nu + E_{th}(AB) = E_i(AB^+) + KE(e^-) \quad (2)$$

For a given total energy given by the left hand side of eq 2, there will be a distribution of electron energies and the corresponding distribution of ion internal energies. However, in the coincidence experiment, we measure only ions which we detect in coincidence (or delayed coincidence) with energy analyzed electrons. This can be done in the gas phase where single ions and electrons are collected at low total count rates so that the electron and ion from each ionization event are collected before the next ionization event takes place. In this manner, we restrict signals to those ions which have an internal energy equal to $h\nu + E_{th}(AB) - KE(e^-)$.

Two types of PIPECO experiments have been done. In one, the light source has a fixed energy (e.g., the 21.2-eV line of the He I lamp) and ions are collected in coincidence with electrons of various energies selected by an electrostatic energy analyzer.[7-9] In the other PIPECO experiment, the photon source is variable and the ions are always collected in coincidence with zero energy, or so-called threshold electrons.[10-13] In the present work, the latter technique is used.

The experimental data consist of ion time-of-flight (TOF) distributions which are obtained by measuring the time difference between the rapidly detected electron and the more slowly moving ion. All the dynamical information is contained in the TOF distribution because anything which changes the ion kinetic energy is reflected in this TOF distribution. Such changes can be brought about by kinetic energy release in a dissociation, collision with a neutral gas, dissociation during the course of acceleration, etc. The relationship between these dynamical events and the TOF distribution are discussed in more detail in the experimental section. In these three papers, we present results on the kinetic energy release accompanying dissociation and ion lifetime measurements.

A number of ions have already been studied by PIPECO. These include $C_5H_5N^+$,[7] $C_2H_3F^+$,[8] $COCl_2^+$,[9] $C_3H_4^+$,[10] $C_4H_6^+$,[11] $C_6H_6^+$,[12] and others.[6] On the basis of these studies, it has become clear that, if possible, ions often isomerize to more stable isomeric structures. These results have confirmed similar conclusions drawn on the basis of metastable ion studies in conventional mass spectrometers. In addition, PIPECO studies have shown that ion lifetimes are often well characterized by the statistical theory (RRKM/QET), although there are dramatic exceptions.[9,14] Finally PIPECO studies have provided essential information for determining ion structures.

We undertook the study of the dissociation of $C_4H_4X^+$, X = S, O, and NH ions, in order to learn more about ion-dissociation dynamics in medium-sized molecules where there is some hope of understanding the dissociation mechanisms. In addition, these investigations also provide information about the molecular ion, transition state, and product ion structures. Finally, we had hoped that a comparison among thiophene, furan, and pyrrole might help us in drawing conclusions about ion structures and dynamics. This last hope proved to be futile because the three ions were remarkably different.

The first study of the ionic fragmentation patterns of thiophene was performed by Khvostenko,[15] who reported the formation of $C_4H_4S^+$, $C_2H_2S^+$, CHS^+, and $C_3H_3^+$ between 9 and 13 eV by using electron impact ionization. In a later study, Derrick et al.[16] examined the ionic fragmentation patterns of thiophene by charge exchange by using primary ions of various recombination energies. They determined crude onsets for the following fragment ions: $C_2H_2S^+$, CHS^+, $C_3H_3^+$, $C_4H_3S^+$, and C_3HS^+.

In the mass spectrum of thiophene, a metastable peak is seen for the fragmentation

$$C_4H_4S^+ \rightarrow C_2H_2S^+ + C_2H_2$$

Andlauer and Ottinger[17] measured the rate of this fragmentation process as a function of the $C_4H_4S^+$ internal energy by preparing the $C_4H_4S^+$ ion by charge exchange with various primary ions. The rates obtained by such charge-exchange studies have been compared to those measured by coincidence methods for HCN loss from $C_6H_5CN^+$[18] and C_2H_2 and C_3H_3 loss from $C_6H_6^+$.[12,18] In both cases, the charge-exchange method gave rates which were approximately a factor of 5 higher.

The nature of the transition state in the fragmentation of thiophene ion to $C_2H_2S^+$ has been the object of much study by mass spectroscopists. Wynberg et al.[19] first proposed the "Ladenburg" structure (I) as a possible, transition state or intermediate in the formation of $C_2H_2S^+$ from thiophene. Siegel[20] and DeJong et al.[21] using ^{13}C-labeled and D-labeled thiophene examined the $C_2H_2S^+$ fragment for isotopic labeling. Both studies

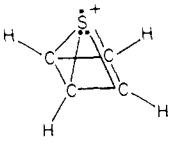

I

(4) W. Forst, "Theory of Unimolecular Reactions", Academic Press, New York, 1973.
(5) H. M. Rosenstock, K. Draxl, B. W. Steiner, and J. T. Herron, *J. Phys. Chem. Ref. Data*, **6** (1) (1977).
(6) T. Baer in "Gas Phase Ion Chemistry", M. Bowers, Ed., Academic Press, New York, 1975, Chapter 5.
(7) J. H. D. Eland, J. Berkowitz, H. Schulte, and R. Frey, *Int. J. Mass Spectrom. Ion Phys.*, **28**, 297 (1978).
(8) J. Dannacher, A. Schmelzer, J. P. Stadelmann, and J. Vogt, *Int. J. Mass Spectrom. Ion Phys.*, **31**, 175 (1979).
(9) K. M. Johnson, I. Powis, and C. J. Danby, *Int. J. Mass Spectrom. Ion Phys.*, **32**, 1 (1979).
(10) (a) A. C. Parr, A. J. Jason, and R. Stockbauer, *Int. J. Mass Spectrom. Ion Phys.*, **26**, 23 (1978); **33**, 243 (1980); (b) A. C. Parr, A. J. Jason, R. Stockbauer, and K. E. McCulloh, *ibid.*, **30**, 319 (1979).
(11) A. S. Werner and T. Baer, *J. Chem. Phys.*, **62**, 2900 (1975).
(12) T. Baer, G. D. Willett, D. Smith, and J. S. Phillips, *J. Chem. Phys.*, **70**, 4076 (1979).
(13) P. M. Guyon, T. Baer, L. F. A. Ferreira, I. Nenner, A. Tabché-Fouhaille, R. Botter, and T. R. Govers, *J. Phys. B*, **11**, L141 (1978).
(14) B. P. Tsai, A. S. Werner, and T. Baer, *J. Chem. Phys.*, **63**, 4384 (1975).
(15) V. I. Khvostenko, *Russ. J. Phys. Chem.* (*Engl. Transl.*), **36**, 197 (1962).
(16) P. J. Derrick, L. Asbrink, O. Edqvist, B-Ö Jonsson, and E. Lindholm, *Int. J. Mass Spectrom. Ion Phys.*, **6**, 177 (1971).
(17) B. Andlauer and C. Ottinger, *Z. Naturforsch., A*, **A27**, 293 (1972).
(18) J. H. D. Eland and H. Schulte, *J. Chem. Phys.*, **62**, 3835 (1975).
(19) H. Wynberg, R. M. Kellogg, H. VanDriel, and G. E. Berkhuis, *J. Am. Chem. Soc.*, **89**, 3501 (1967).
(20) A. S. Siegel, *Tetrahedron Lett.*, **47**, 4113 (1970).
(21) F. de Jong, H. J. M. Sinnige, and M. J. Janssen, *Org. Mass Spectrom.*, **3**, 1539 (1970).

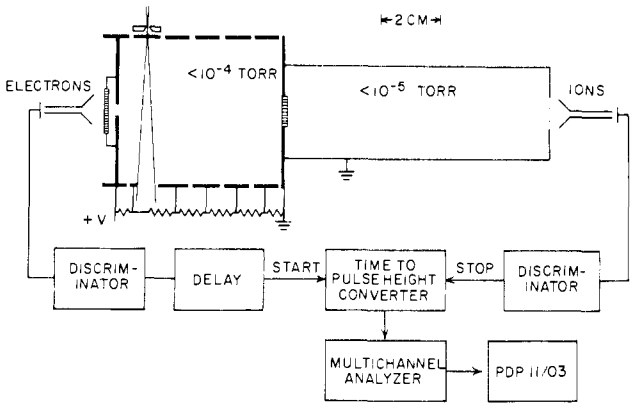

Figure 1. Diagram of the photoion–photoelectron coincidence experiment.

were consistent with the "Ladenburg" transition state.

Experimental Section

The PIPECO spectrometer used in these experiments to record threshold photoelectron spectra, photoionization efficiency curves, and coincidence time-of-flight spectra is an improved version of an instrument described in detail previously.[11] The ionizing radiation is UV light from a hydrogen many line source dispersed by a 1-m normal incidence monochromator with a wavelength resolution of 2 Å (18 meV at 12-eV photon energy). The light enters a pressurized ionization/acceleration region shown in Figure 1. Ions and electrons are accelerated in opposite directions by the applied DC electric field. Zero kinetic energy electrons are selected by a steradiancy analyzer[22] consisting of a set of collimated holes with length to diameter ratio of 40. Such an analyzer is essentially a filter which rejects energetic electrons with initial velocity components perpendicular to the electric field because they hit walls or apertures. Such analysers do not discriminate against energetic electrons ejected parallel to the hole axes. However, it is possible to use electron time-of-flight (TOF) analysis to eliminate this hot electron contribution.[23] The threshold photoelectron spectra were recorded in this manner. However for the coincidence experiment, a DC field was used so that the coincidence results contain some contribution from lower energy ions.

Threshold photoelectron spectra (TPES) are obtained by collecting zero-energy electrons as a function of the photon energy. Whenever the photon energy is in resonance with an ion state, threshold electrons are produced. Their intensity is determined by Franck–Condon factors and electronic transition moments. The TPES are very similar to normal He I PES except that the intensities are often perturbed by superexcited neutral states (autoionizing states) which give added intensity to the ionization process. This has the effect of allowing the production and selection of ion states in very high vibrational levels by the threshold electron technique.

In the electric field of the ionization region, ions are accelerated in a direction opposite to that of the electrons. Ions also pass through a set of stainless collimated holes (length/diameter ratio of 10) which serve to pressurize the ion source. The 9-cm long drift distance completes an ion TOF mass spectrometer with unit mass resolution for an m/e 20 at a draw out voltage of 60 V. This is sufficient for mass analysis of some fragments. However, a quadrupole mass filter was substituted for the drift region when measuring photoionization efficiency curves for the various masses. The mass filter was also used in some of the coincidence studies when a resolution greater than 20 was required. Unfortunately, the quadrupole adds instrumental broadening to the ion TOF distributions, thereby making the analysis of ion dynamics less precise.

In the coincidence experiment, the internal energy of the parent ions are selected by collecting only those fragment ions which are associated with zero-energy electrons. In practice, this is accomplished by utilizing the electron and ion signals as start and stop inputs, respectively, to a time-to-pulse height converter (Figure 1). The output from the latter is fed into a multichannel pulse height analyzer which then displays the ion time-of-flight (TOF) distribution resulting from parent ions of a specific internal energy.

All the dynamical information is contained in the fragment ion TOF distribution. Kinetic energy released in the fragmentation processes

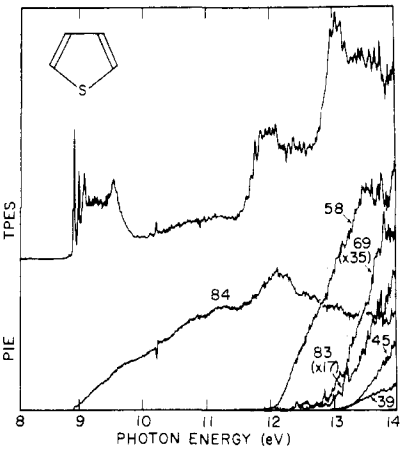

Figure 2. Threshold photoelectron spectrum (TPES) of thiophene and the photoionization efficiency (PIE) curves for $C_4H_4S^+$ (m/e 84), $C_4H_3S^+$ (m/e 83), C_3HS^+ (m/e 69), $C_2H_2S^+$ (m/e 58), CHS^+ (m/e 45), and $C_3H_3^+$ (m/e 39).

results in symmetrically broadened TOF peaks whose widths can be related to the average kinetic energy release.[12,24] More detailed analyses can yield the distribution of release energies.[25,26] Metastable ions whose mean lifetimes are between 10^{-4} and 10^{-7} s fragment at various positions in the acceleration region between the point of ionization and the drift region. The TOF of fragments which result from such long-lived precursor ions is given by eq 3 in which the subscripts a and d refer to

$$\mathrm{TOF} = T_a(\mathrm{parent}) + T_a(\mathrm{fragment}) + T_d(\mathrm{fragment}) \qquad (3)$$

acceleration and drift regions, respectively. The longer the ion lifetime, the further the parent ion travels in the acceleration region and the longer will be the resulting fragment ion time-of-flight. This results in asymmetric fragment ion TOF distributions from which the mean lifetime, or decay rate, can be extracted.[11,12] At low ion internal energy, the kinetic energy released will be small but the lifetime is long. At high internal energies, the reverse is true. Thus, we generally analyze for the kinetic energy release at high ion internal energy and for the ion lifetime at low parent ion internal energy.

Results

(A) Threshold Photoelectron Spectrum. The threshold photoelectron spectrum (TPES) of thiophene is illustrated in Figure 2. Our ionization energy is 8.87 ± 0.01 eV. The He I photoelectron spectrum of thiophene was measured by Eland[27] and Derrick et al.,[16] and in both studies an ionization energy of 8.87 eV was found. The first three bands with vertical ionization energies of 8.9, 9.5, and 12.1 eV have been assigned[16] as originating from the π-electron system of thiophene. These bands are evident in the TPES of Figure 2.

There is considerable electron signal between the second and third bands (10–11.5 eV) in the TPES. This type of structure has been reported for a number of molecules by Murray and Baer[23] and has been associated with resonant autoionization which forms ions in high vibrationally excited states. Autoionization is a two-step ionization process in which the molecule is first excited to a metastable neutral molecule which then ejects its electron in typically 10^{-10}–10^{-13} s.

(B) Photoionization Efficiency Curves. The photoionization efficiency curves for the parent thiophene ion and five fragment ions are shown in Figure 2. The parent ion signal (mass 84) continues to rise between 10 and 12 eV, as a result of the previously mentioned autoionization of Rydberg states converging to the ion state at 12 eV. Still more convincing evidence for autoionization is the peak for mass 84 just above 12 eV. Most likely this peak

(22) T. Baer, W. B. Peatman, and E. W. Schlag, *Chem. Phys. Lett.*, **4**, 243 (1969).
(23) P. T. Murray and T. Baer, *Int. J. Mass Spectrom. Ion Phys.*, **30**, 155 (1979).
(24) R. Stockbauer, *Int. J. Mass Spectrom. Ion Phys.*, **25**, 89 (1977).
(25) D. Mintz and T. Baer, *J. Chem. Phys.*, **65**, 2407 (1976).
(26) I. Powis and C. J. Danby, *Chem. Phys. Lett.*, **65**, 390 (1979).
(27) J. H. D. Eland, *Int. J. Mass Spectrom. Ion Phys.*, **2**, 471 (1969).
(28) S. W. Benson, "Thermochemical Kientics", Wiley, New York, 1976.
(29) F. P. Lossing, *Can. J. Chem.*, **50**, 3973 (1972).
(30) W. Tsang, *Int. J. Chem. Kinet.*, **2**, 23 (1970).

Table I. Appearance Energies and Heats of Formation of Various Sulfur-Containing Ions and Radicals from Thiopene

products	appearance energy,[a] eV	derived $\Delta H_f^\circ{}_{(298)}$,[d] kcal/mol
$C_4H_4S^+$	8.87 ± 0.01, 8.872,[b] 9.2 ± 0.2[c]	$C_4H_4S^+$ (232.1 ± 0.2)
$C_2H_2S^+ + C_2H_2$	12.1 ± 0.1, 11.5,[b] 10.8 ± 0.2[c]	$C_2H_2S^+$ (253 ± 2)
$C_4H_3S^+ + H$	12.93 ± 0.07, 12.4[b]	$C_4H_3S^+$ (<274 ± 2.0)
$C_3HS^+ + CH_3$	12.95 ± 0.05, 13.7[b]	C_3HS^+ (<292 ± 3.0)
$C_3H_3^+ + CHS$	13.06 ± 0.05, 13.0,[b] 12.8 ± 0.2[c]	CHS (<73 ± 2)
$CHS^+ + C_3H_3$	13.19 ± 0.04, 13.0,[b] 13.0 ± 0.2[c]	CHS^+ (<251 ± 2)

[a] Unreferenced results are from this study. [b] Reference 16. [c] Reference 15. [d] The following heats of formation were assumed: C_4H_4S (27.66);[5] C_2H_2 (54.19);[5] H (52.95);[5] CH_3 (34.0);[28] $C_3H_3^+$ (256);[29] C_3H_3 (80.7).[30]

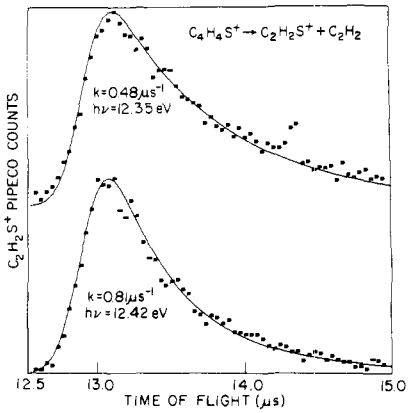

Figure 3. Time-of-flight (TOF) spectra for the $C_2H_2S^+$ ion at two different photon energies in the metastable region.

results from a number of closely spaced Rydberg states converging to the ion state at 13 eV.

All the fragment ions have appearance energies in regions of high transition probabilities. These are summarized in Table I, along with derived heats of formation for the various ionic and neutral fragments. These heats of formation are obtained from the relation: $\Delta H_f^\circ(AB)$ + appearance energy = $\Delta H_f^\circ(A^+)$ + $\Delta H_f^\circ(B)$. To our knowledge, the fragment ion and neutral heats of formation in column 3 are the first reliable measurements for these fragments. The appearance energies provide us only with upper limits to the thermodynamic dissociation limits because of such factors as reverse activation energy and kinetic shift. The latter quantity arises, for the case of the first fragment, from decay rates at threshold which are too slow to allow a sufficient number of ions to fragment during the few microseconds collection time. In favorable circumstances, this kinetic shift can be determined by measuring the decay rates and comparing them with calculated rates (statistical theory). The kinetic shifts for the higher energy fragments arise from the competitive decay rates between the various fragments. The magnitudes of these shifts are very difficult to determine because the mechanism for dissociation at higher energies is often unknown. Because of these uncertainties, some of the derived heats of formation are listed only as upper limits in Table I.

(C) Unimolecular Decay Rates. Only one fragment ion, $C_2H_2S^+$, is formed in the metastable energy region between 12.1 and 12.7 eV. Typical TOF spectra at two different photon energies together with their corresponding calculated curves are shown in Figure 3. Counting times to obtain these TOF curves were 3 and 5 h. The solid TOF curves in Figure 3 are calculations based on a single unimolecular decay. Parameters fixed by the experiment and used in the calculation are the acceleration and drift distances, the applied voltage across the ionization region, and the parent and daughter ion masses. The only adjustable parameter in the calculation is the decay rate. The calculated TOF

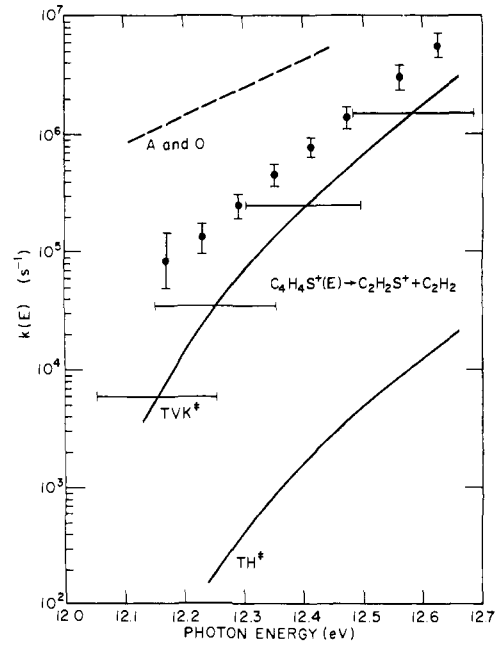

Figure 4. A plot of the decay rate, $k(E)$, as a function of photon energy for the dissociation of thiophene ion to $C_2H_2S^+$ and C_2H_2. The two solid curves are the results of RRKM calculations assuming a thiophene (TH‡) transition state and a thiovinyl ketene (TVK‡) transition state. The dashed line represents the results of a previous study of Andlauer and Ottinger.[17]

distributions are convoluted by a Gaussian function to take into account the thermal broadening of the experimental TOF distributions.

Figure 4 is a plot of the derived decay rates as a function of photon energy. The Andlauer and Ottinger[17] data are also shown in this figure as well as the results of statistical theory (RRKM) calculations. The disagreement between the experimental data of this study and those of Andlauer and Ottinger is substantial.

Before the $k(E)$ vs. E curve of Figure 4 can be compared to the calculated rates, it is necessary to know the onset for $C_2H_2S^+$ formation. Because of the extremely slow dissociation, we, in fact, cannot obtain the true onset from Figure 2. However, the kinetic energy release methods discussed in the following section provide us with a good estimate of the onset.

(D) Average Kinetic Energy Released upon Fragmentation. The $C_2H_2S^+$ fragment ion TOF distributions in the photon energy range between 13 and 14 eV were analyzed for the average kinetic energy released upon fragmentation. The $C_2H_2S^+$ ion TOF distributions were Gaussian in shape in this energy range above the metastable region. The full width at half-maximum (fwhm) of each TOF distribution was obtained by a nonlinear least-squares fit of a Gaussian curve to the TOF distribution. The average kinetic energy released was calculated from the fwhm by using eq 4 taken from Stockbauer[24] in which M and m are the parent and daughter ion masses, respectively, q is the electron charge, and ϵ is the electric field strength.

$$\langle T \rangle = \frac{3M}{15(\ln 2)m(M-m)}(q\epsilon)^2\,(\text{fwhm})^2 - \frac{3RT}{2}\frac{m}{(M-m)} \quad (4)$$

Figure 5 is a plot of the experimentally determined average kinetic energy released as a function of photon energy. The PIPECO experiment does not yield kinetic energy release values close to the dissociation limit because of the asymmetric TOF distributions (Figure 3). However, kinetic energy release information can be obtained from the complementary experimental approach of mass-analyzed kinetic energy spectroscopy (MIKES).[31] Ions in the MIKES experiment are not state selected except through the relationship between the parent ion internal

(31) This experiment was performed in the laboratory of R. Hass, NIEHS, Research Triangle Park, on a ZAB/2F MIKES spectrometer.

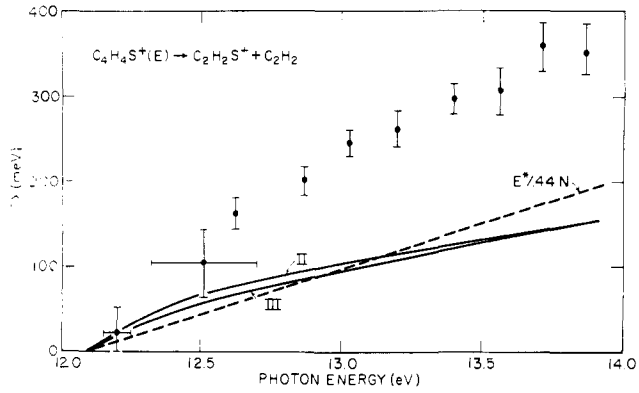

Figure 5. A plot of average kinetic energy released, $\langle T \rangle$, as a function of photon energy for the dissociation of thiophene ions to $C_2H_2S^+$ and C_2H_2. The two low energy points are from a MIKES experiment. Curves II and III are the results of two QET calculations assuming a cyclic and a linear structure of $C_2H_2S^+$, respectively. The dashed line is the calculated curve obtained from the empirical relation $E^*/0.44$ N.

energy and the fragmentation time. By calculating the fragmentation time of the parent ion from a knowledge of the electric and magnetic fields and geometry of the MIKES experiment and using our results from Figure 4, we determined the mean internal energy of the thiophene ions in the MIKES experiment.

Discussion

Figure 5 shows consistent results for average kinetic energy release values determined by PIPECO and MIKES. From this plot, there can be little doubt that the onset for fragmentation is at 12.1 ± 0.1 eV. In addition, the fact that the kinetic energy release values go to zero suggests that there is no reverse activation barrier for the formation of $C_2H_2S^+ + C_2H_2$. The onset can therefore be used to calculate a heat of formation at 298 K of $C_2H_2S^+$ of 253 ± 3 kcal/mol.

Included in Figure 5 are the results of a calculation using the quasi-equilibrium theory (QET) as formulated by Klots[32-34] in terms of the final states of the separated fragments and the Langevin collision model for the reverse association reaction. The result is in the form of eq 5 in which R is the number of internal

$$E = \frac{(R+1)}{2}\langle T \rangle + \sum_i h\nu_i[\exp(h\nu_i/\langle T \rangle)^{-1}]^{-1} \qquad (5)$$

rotational degrees of freedom of the products, ν_i are the neutral product and fragment ion vibrational frequencies, E is the total energy above the dissociation limit, and $\langle T \rangle$ is the average kinetic energy released. The QET calculation was performed for both the cyclic and linear fragment ion structures shown below. Clearly we cannot distinguish which structure, II or III, is more reasonable on the basis of the kinetic energy release results.

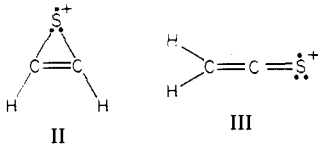

II III

Haney and Franklin's empirical relation[35] for the kinetic energy release $\langle T \rangle = E^*/0.44$ N, in which E^* is the energy above the dissociation limit and N is the number of vibrational degrees of freedom of the parent ion, is included in Figure 5. Both the QET and empirical relation predict average kinetic energy releases that are half the experimental values. A similar disagreement with the QET has been noted for the acetone ion dissociation.[6] It suggests that the available energy is not being distributed to all vibrational modes of the ion but rather is confined to a subset of the modes prior to dissociation. Alternatively, the point particle assumption of the Langevin model may be a poor approximation for the dissociation of two very nonspherical fragments.

Table II. Vibrational Frequencies (in cm^{-1}) of Thiophene and Thiovinyl Ketene Used in RRKM Calculations

thiophene[a]	3126, 3125, 3098, 3086, 1504, 1409, 1360, 1256, 1085, 1083, 1036, 903, 872, 867, 839, 751, 712, 688, 608, 567, 452
thiovinyl ketene[b]	3118, 3103, 3028, 3000, 1907, 1630, 1596, 1420, 1275, 1275, 1158, 993, 993, 959, 912, 770, 450, 370, 307, 137, 89

[a] Reference 30. [b] Frequencies constructed from $CH_2{=}CH_2$ and $CH_2C{=}O$ frequencies found in ref 39 and 40, respectively.

The onset for $C_2H_2S^+$ from Figure 5 allows us to calculate the statistically expected $k(E)$ vs. E curve of Figure 4. Included in Figure 4 are the results of two RRKM calculations (eq 1) corresponding to two different transition states.

The ionization which produces a thiophene ion at 12 eV removes a lower lying π electron, leaving the ion electronically excited. In the ion lifetime calculations, we have assumed that the excited ion undergoes a rapid radiationless transition to the ground electronic state. This is consistent with the behavior of many metastable ions studied so far.

In evaluating the decay rate by eq 1, we must assume vibrational frequencies and moments of inertia for the molecular ion and the transition state. The Hase-Bunker program[36] was used in these calculations with the semiclassical Whitten-Rabinovitch[37] state counting option. The molecular ion frequencies were assumed to be those of neutral thiophene. The two sets of transition-state frequencies used were those of thiophene (structure IV) and the linear thiovinyl ketene (structure V). The thiovinyl ketene

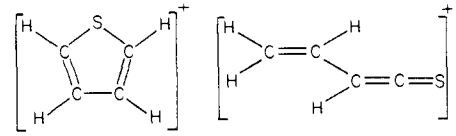

IV V

structure was chosen because the vinyl ketene ion is known to be quite stable.[38] Neither of these structures should be taken too seriously as being *the* transition state. They merely represent two extreme transition states, the former a tight one, the latter a loose one. The terms tight and loose are equivalents to low and high entropy. The thiovinyl ketene has one free, or nearly free, rotation and other low vibrational frequencies, giving it a high entropy of activation.

The frequencies for the thiovinyl ketene were generated by appropriately combining the frequencies of a number of functional groups of thiovinyl ketene. These along with the frequencies of thiophene[39] are listed in Table II. The loose transition state results in calculated rates which are consistent with our experimental data. The "Ladenburg" structure I would have even higher frequencies than those of thiophene and would therefore have RRKM rates which are even lower.

Both calculations and our data disagree with the experimental results of Andlauer and Ottinger. We can offer no explanation for the discrepancy of the two experimental results. However in support of our data, we can claim excellent agreement between our decay rates of other ions with those measured by other workers. These include the dissociation of benzene[12,18] and butadiene[11,41] ions. The agreement between our dissociation rates of chlorobenzene[42] and those recently determined by Rosenstock et al.[43]

(32) C. E. Klots, *J. Chem. Phys.*, **58**, 5364 (1973).
(33) C. E. Klots, *Adv. Mass Spectrom.*, **6**, 969 (1974).
(34) C. E. Klots, *J. Chem. Phys.*, **64**, 4269 (1976).
(35) M. A. Haney and J. L. Franklin, *J. Chem. Phys.*, **48**, 4903 (1968).
(36) Available as program 234 through the Quantum Chemistry Exchange, Indiana University.
(37) G. Z. Whitten and B. S. Rabinovitch, *J. Chem. Phys.*, **41**, 1883 (1964).
(38) J. K. Terlouw, P. C. Burgers, and J. L. Holmes, *J. Am. Chem. Soc.*, **101**, 225 (1979).
(39) T. Shimanouchi, *Natl. Stand. Ref. Data Ser. (U.S., Natl. Bur. Stand.)*, **39** (1972).
(40) A. P. Cox and A. S. Esbitt, *J. Chem. Phys.*, **38**, 1636 (1963).
(41) J. Dannacher, to be submitted for publication.
(42) T. Baer, B. P. Tsai, D. Smith, and P. T. Murray, *J. Chem. Phys.*, **64**, 2460 (1976).

is less satisfactory. No explanation for the latter discrepancy has been advanced.

The facts that the average kinetic energy release values indicate that there is little or no reverse activation barrier for dissociation of thiophene to $C_2H_2S^+$ and C_2H_2, and the loose thiovinyl ketene transition state as indicated by the RRKM calculations leads us to postulate linear structure III for the $C_2H_2S^+$ fragment. In order to investigate this further, we performed ab initio calculations by using a Gaussian 70 program with the extended splitvalence 4-31G basis set[44] on the linear and cyclic structures for $C_2H_2S^+$. By optimizing geometries for the two structures, we found total energy minima for both structures. These calculations indicate that the linear structure is indeed more stable than its cyclic counterpart by 1.1 eV. This is contrary to previously assumed cyclic structure (II) of $C_2H_2S^+$.[45]

The possibility that the thiophene parent ion isomerizes to a more stable linear structure was considered. Two points argue against such a structure. First, ab initio calculations on the thiophene and thiovinyl ketene structures indicate that the thiophene ion is far more stable than the thiovinyl ketene ion. Second, a lower parent ion energy would have the effect of raising the activation energy, thereby increasing the parent ion density of states (denominator in eq 1). In addition, the lower vibrational frequencies of a linear structure would further increase the density of states. The net result would be to lower the RRKM calculated rate by over 2 orders of magnitude, contrary to the experimental results.

(43) H. M. Rosenstock, R. Stockbauer, and A. C. Parr, *J. Chem. Phys.*, **71**, 3708 (1979).
(44) R. Ditchfield, W. J. Hehre, and J. A. Pople, *J. Chem. Phys.*, **54**, 724 (1971). QCPE program No. 234.
(45) H. Budzikiewicz, C. Djerassi, and D. H. Williams, "Mass Spectrometry of Organic Compounds", Holden-Day, San Francisco, 1967.

Conclusion

A thermochemical onset for the dissociation of $C_4H_4S^+$ to $C_2H_2S^+$ and C_2H_2 measured by the kinetic energy release as a function of excess $C_4H_4S^+$ internal energy has been used to establish a 298 K heat of formation of the $C_2H_2S^+$ ion of 253 ± 3 kcal/mol. Comparison of the experimentally determined decay rates as a function of $C_4H_4S^+$ internal energy with calculated rates based on the statistical RRKM theory indicates that the parent ion structure is that of thiophene while the transition state is a loose structure such as thiovinyl ketene. Under these assumptions, there is excellent agreement between experimentally measured and the RRKM-calculated decay rates. These rates are significantly lower than those measured by Andlauer and Ottinger. The average kinetic energy releases as a function of ion internal energy increase monotonically with energy as expected on the basis of the statistical theory. However, the magnitude is significantly greater than predicted.

Acknowledgment. This work received support from the National Science Foundation. We thank Dr. Ron Hass for providing us with the MIKES kinetic energy release data.

Thermochemistry and Dissociation Dynamics of State-Selected C_4H_4X Ions. 2. Furan and 3-Butyn-2-one

Gary D. Willett[1] and Tomas Baer*

Contribution from the Department of Chemistry, The University of North Carolina at Chapel Hill, Chapel Hill, North Carolina 27514. *Received January 31, 1980*

Abstract: The photoion-photoelectron coincidence technique has been used to investigate the unimolecular decomposition mechanism of metastable state-selected furan and 3-butyn-2-one ions. Threshold photoelectron spectra and photoionization efficiency curves for the various fragment ions as well as fragment ion time-of-flight distributions are presented. From a comparison of the measured and statistically calculated absolute unimolecular dissociation rates, together with evidence from an independent study on the kinetic energy releases of a variety of $C_4H_4O^+$ isomers, it is concluded that at low internal energies the furan ion dissociates to $C_3H_4^+$, $C_2H_2O^+$, and $C_3H_3^+$ directly or possibly via a rate-determining isomerization. It is further shown that 3-butyn-2-one(1+) dissociates directly without first isomerizing to the more stable furan(1+) ion. The first and major product is $CHCCO^+$ whose ΔH_{f298K} is calculated to be 232 kcal mol^{-1}. Gaussian 70 4-31G ab initio MO calculations have been used to calculate the relative stabilities of various $C_4H_4O^+$ and $C_2H_2O^+$ structures.

I. Introduction

In 1971, Derrick et al.[2] reported the charge-exchange mass spectra of furan for primary ions of several recombination energies. In that experiment, charge transfer between a simple ion and the furan molecule results in the production of energy-selected furan ions. That study established that in the energy range 11-12 eV furan dissociates via three paths which are

$$C_4H_4O^+ \rightarrow C_3H_4^+ + CO \quad (1)$$

$$C_4H_4O^+ \rightarrow C_2H_2O^+ + C_2H_2 \quad (2)$$

$$C_4H_4O^+ \rightarrow C_3H_3^+ + CHO \quad (3)$$

Other reaction products observed at higher energy were $C_4H_3O^+$ and HCO^+.

In the charge-transfer preparation, ions are formed in relatively narrow and well-determined internal energies. For this reason, the charge-transfer mass spectra as a function of the ionizing energy constitute a breakdown diagram, which gives directly the relative rates for dissociation to the various fragments as a function of the parent ion internal energy. Insight into the dissociation dynamics can often be obtained by comparing experimental breakdown diagrams to those predicted by a theory, particularly the statistical theory of unimolecular decay (RRKM[3a] or QET[3b]). The input required for such calculations are dissociation onsets and vibrational frequencies and moments of inertia of the mo-

(1) Commonwealth Scientific Industrial Research Organization Postdoctoral Research Fellow, 1978.
(2) P. J. Derrick, L. Åsbrink, O. Edquist, B.-Ö. Jonsson, and E. Lindholm, *Int. J. Mass Spectrom. Ion Phys.*, **6**, 161 (1971).
(3) (a) R. A. Marcus and O. K. Rice, *J. Phys. Colloid Chem.*, **55**, 894 (1951); (b) H. B. Rosenstock, M. B. Wallenstein, A. L. Wahrhaftig, and H. Eyring, *Proc. Natl. Acad. Sci. U.S.A.*, **38**, 667 (1952).

0002-7863/80/1502-6769$01.00/0